Ultraviolet emissions excited by accelerated electrons

P.-N. Ni,[1,2] C.-X. Shan,[1,3] S.-P. Wang,[1] B.-H. Li,[1] Z.-Z. Zhang,[1] and D.-Z. Shen[1,4]

[1]State Key Laboratory of Luminescence and Applications, Changchun Institute of Optics, Fine Mechanics and Physics, Chinese Academy of Sciences, Changchun 130033, China

[2]Graduate University of the Chinese Academy of Sciences, Beijing 100049, China

[3]e-mail: phycxshan@yahoo.com.cn

[4]e-mail: shendz@ciomp.ac.cn

Received January 3, 2012; revised February 20, 2012; accepted March 9, 2012; posted March 13, 2012 (Doc. ID 160900); published May 2, 2012

By employing an insulating zinc oxide (*i*-ZnO) as an electron accelerating layer, and an *n*-type ZnO as an active layer, ultraviolet (UV) emissions at 385 nm caused by the excitation of the *n*-ZnO layer by the accelerated electrons from the *i*-ZnO layer have been realized. By replacing the active layer with larger bandgap $Mg_{0.39}Zn_{0.61}O$ and properly optimizing the structure, shorter wavelength emissions at around 328 nm have been obtained. Considering that the *p*-type doping of wide bandgap semiconductors is still a challenging issue, the results reported in this Letter may provide a promising alternative route to UV emissions. © 2012 Optical Society of America

OCIS codes: 160.0160, 230.3670, 250.1500, 310.6845, 260.7190.

Wide bandgap semiconductor based ultraviolet (UV) emissions have a wide range of applications including solid-state lighting, food sterilization, water and air purification, etc. [1,2]. Nevertheless, although great progress has been witnessed in the past decades [3,4], the *p*-type doping of wide bandgap semiconductors is still challenging due to the strong compensation and relatively large activation energy of acceptors [5–7], which makes *pn* junction based short-wavelength emissions problematic. Historically, the electron-beam has been widely employed to excite phosphors for lighting and displaying [8–10]. Inspired by the great success that has been achieved in electron-beam excited visible emission, it is believed to be a promising way to realize UV emissions under the excitation of electron-beam. Recently, some groups have demonstrated UV emissions by employing electron-beam as the excitation source [11–13]. It is commented that electron-beam excitation may promise the realization of high-power efficient semiconductor-based deep UV emission by bypassing the challenging *p*-type doping of wide bandgap semiconductors [14]. Nevertheless, traditionally, the electron-beam was generated in a vacuum atmosphere at high voltage, which makes the facility bulky and costly. Although, Watanabe *et al.* demonstrated a handheld electron-beam source [12], a vacuum chamber is still a necessity for the device, which impairs the usefulness of the device. If electron-beam excited UV emissions can be realized in a neat sized solid-state device, it will be of great significance and importance. However, although some reports on visible emissions excited by electron-beams in solid-state structure have been demonstrated [15–18], no such report on UV emissions can be found up to now.

In this Letter, a light-emitting structure has been designed and fabricated from insulating zinc oxide/*n*-type zinc oxide (*i*–ZnO/*n*–ZnO). Under reverse bias, the electrons in the *i*-ZnO will be accelerated greatly due to the relatively large electric field in this layer, and will excite the *n*-ZnO layer; in this way UV emissions have been obtained. Meanwhile by employing larger bandgap magnesium zinc oxide (MgZnO) as the active layer, shorter wavelength UV emission at around 328 nm has been realized.

To fabricate the *i*–ZnO/*n*–ZnO structure, a 300 nm ZnO film was first deposited using a VG V80H plasma-assisted molecular-beam epitaxy. The as grown ZnO film shows *n*-type conduction with an electron concentration of 4.2×10^{17} cm^{-3} and a Hall mobility of 46 $cm^2\,V^{-1}s^{-1}$. Then a 160 nm insulating ZnO (*i*-ZnO) film, of which the resistivity is too high to be measured by our Hall measurement system, was deposited onto the *n*-ZnO layer in a radio frequency magnetron sputtering technique. Then an Au layer and an In layer were deposited onto the *i*-ZnO and *n*-ZnO layer by vacuum evaporation, respectively, acting as electrodes. For shorter wavelength emissions, a MgZnO/MgO/*n*–ZnO structure has been designed and fabricated. In this structure, a 630 nm ZnO film acting as an electron source was grown on *a*-plane sapphire, followed by a 100 nm MgO electron-accelerating layer. Finally, a 200 nm MgZnO active layer was grown onto the MgO layer. A semitransparent thin Au film was deposited onto the MgZnO and an In contact onto the ZnO layer in vacuum evaporation acting as electrodes.

The electrical properties of these films of the structures were characterized in a Hall measurement system (LakeShore 7707), and the current-voltage (*I*–*V*) characteristics were measured using a Keithley 2611A System SourceMeter. The Mg content in the MgZnO layer was determined to be 0.39 by energy-dispersive x-ray spectroscopy. The emissions of the structures were collected in a Hitachi F4500 spectrometer.

The inset of Fig. 1 shows the schematic diagram and emission recording geometry of the *i*–ZnO/*n*–ZnO structure. The *I*–*V* characteristics of the structure are shown in Fig. 1, where the reverse bias is defined as the situation that the negative voltage is applied on the Au contact. There appears a weak rectifying behavior in this structure at both forward and reverse bias region. Under reverse bias, due to the different conductive nature between the *i*-ZnO and *n*-ZnO, most of the voltage will be applied onto the *i*-ZnO layer. Considering that the thickness of the *i*-ZnO layer is only about 160 nm, the electric field in the *i*-ZnO will be very high, e.g., it will be as high as 2.8×10^6 V/cm at 45 V bias. Thus, when the electrons coming from the Au electrode move into this layer, they will be accelerated greatly by such a high field and gain

 © 2012 Optical Society of America

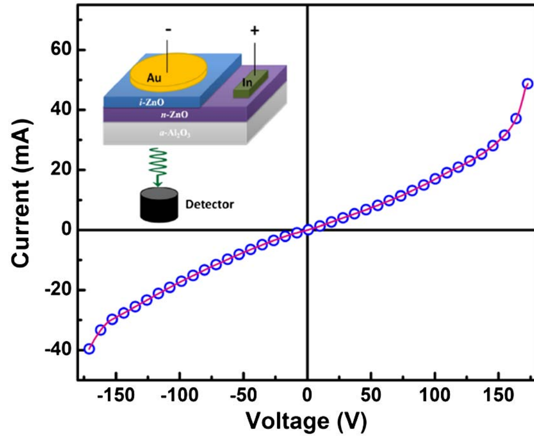

Fig. 1. (Color online) Current—voltage characteristics of the i–ZnO/n–ZnO structure, and the inset shows the schematic diagram and emission recording geometry of the structure.

much kinetic energy. Once these accelerated electrons enter into the n-ZnO layer, they will release their energy by exciting the electrons in the valence band of the n-ZnO into its conduction band, giving rise to free electrons and holes. Then the electrons in the conduction band of n-ZnO will recombine with the generated holes in the valence band, as a result, UV emissions will be realized.

To test the feasibility of the above-mentioned accelerated electron excited UV emissions, a reverse bias was applied onto the i–ZnO/n–ZnO structure. Obvious UV emissions have been observed from the structure, as shown in Fig. 2. As can be seen, under the reverse bias of 45 V, an emission at around 385 nm is clearly visible from the n-ZnO side, which can be attributed to the near-band-edge (NBE) emission of the n-ZnO layer, while the deep-level emission is almost undetectable. The inset of Fig. 2 shows the integrated intensity of the emission at around 385 nm as a function of the applied reverse bias. As evidenced from the figure, the UV emission intensity increases significantly with increasing the reverse bias. The obvious emissions confirm that the accelerated electrons obtained in this structure can be used to excite wide bandgap semiconductors for UV emissions.

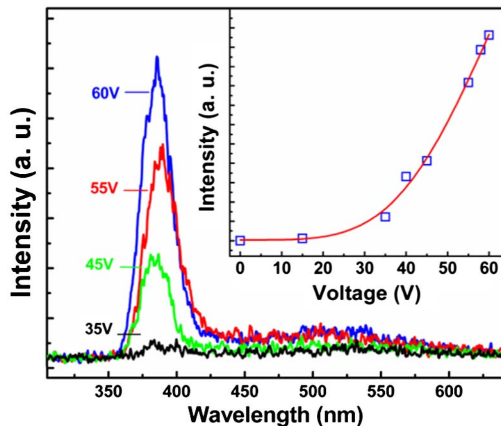

Fig. 2. (Color online) Emission spectra of i–ZnO/n–ZnO structure under different reverse bias, and the inset shows the integrated intensity of UV emissions at around 385 nm as a function of the reverse bias voltage.

Considering that the accelerated electrons can be easily obtained via the above-mentioned process and used to excite ZnO to realize UV emissions, it will be of greater significance if shorter wavelength emissions can be realized via this route since the doping of wider bandgap semiconductors is even more challenging. To this end, an $Mg_{0.39}Zn_{0.61}O$/MgO/n–ZnO structure has been designed and fabricated, of which the schematic illustration and the bandgap diagram are shown in Fig. 3. The n-ZnO layer, with an electron concentration and mobility of 2.1×10^{18} cm^{-3} and 68 $cm^2\,V^{-1}\,s^{-1}$, respectively, will act as an electron source for the $Mg_{0.39}Zn_{0.61}O$ active layer. Under the reverse bias where the negative voltage was applied on the In contact, the electrons in the n-ZnO layer will be concentrated at the MgO/ZnO interface due to the large conduction band offset (3.55 eV) between the MgO and ZnO. In this way a region with high surface charge density will form underneath the MgO layer. Considering that most of the bias will be applied onto the MgO layer due to its dielectric nature, the conduction and valence bands of the MgO layer will bend drastically. Then the width of the barrier that hinders the tunnel of the electrons in the n-ZnO to the $Mg_{0.39}Zn_{0.61}O$ layer will be greatly reduced. As a result, many electrons can tunnel through the MgO layer and inject into the $Mg_{0.39}Zn_{0.61}O$ active layer. Note that when the electrons enter into the MgO layer, they will be accelerated greatly due to the large electric field in this layer. Then the accelerated electrons will release their energy by generating free electrons and holes in the $Mg_{0.39}Zn_{0.61}O$ layer. When these generated holes recombine with free electrons, emissions may be obtained. Experimentally, emissions have indeed been observed from the structure under reverse bias, as shown in Fig. 4. Under the reverse bias of 70 V, a broad emission with three bands at about 328 nm, 400 nm, and 598 nm can be observed. The emission at 598 nm may arise from the deep-level emission at the n-ZnO/MgO interface, while the one at around 400 nm corresponds to the NBE emission of the n-ZnO. The broad peak at around 328 nm can be attributed to the NBE emission of the $Mg_{0.39}Zn_{0.61}O$ layer. Note that the NBE emission of the $Mg_{0.39}Zn_{0.61}O$ increases greatly, the NBE emission of n-ZnO hardly changes, and the deep-level emission decreases greatly with increasing the applied voltage. When the reverse bias reaches 96 V, the emission at 328 nm dominates the spectrum, while the

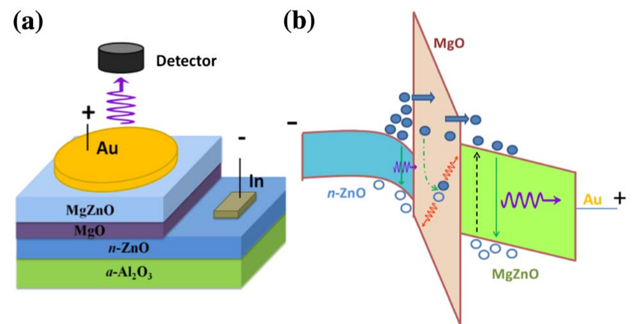

Fig. 3. (Color online) (a) Schematic diagram of the $Mg_{0.39}Zn_{0.61}O$/MgO/n–ZnO structure; (b) Band diagram of the MgZnO/MgO/n–ZnO structure under reverse bias.

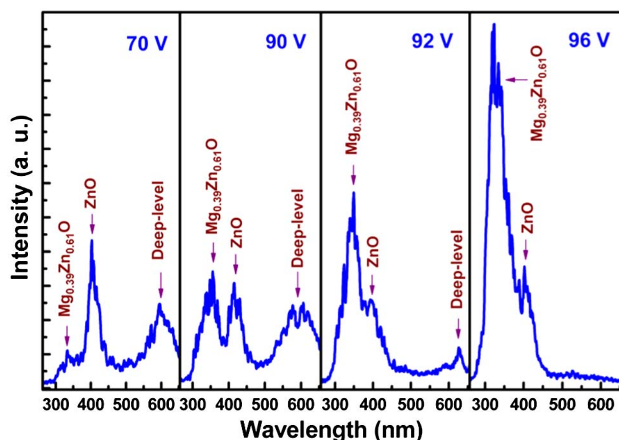

Fig. 4. (Color online) Emission spectra of $Mg_{0.39}Zn_{0.61}O$/MgO/n–ZnO structure under different reverse bias.

NBE emission and deep-level emission of the n-ZnO become very weak.

The above dependence of the emissions on the applied reverse bias can be understood as follows: During the acceleration process, some of the accelerated electrons may impact with the lattice of MgO, thus additional electron-hole pairs will be generated by this impact ionization process [19], and then the generated holes will be injected into the ZnO layer, and recombine radiatively with the electrons accumulated at the ZnO/MgO interface. As a result, the NBE emission and the deep-level emissions of ZnO are observed. While for the generated electrons, they may be further accelerated by the large electric field in the MgO layer. Although the electrons will lose part of their kinetic energy during the impact ionization process, the number of the electrons that can reach the $Mg_{0.39}Zn_{0.61}O$ layer will be increased by this impact ionization process. At moderate bias (e.g., 70 V), only a few electrons will gain enough energy to excite the $Mg_{0.39}Zn_{0.61}O$ layer, so the emission of the $Mg_{0.39}Zn_{0.61}O$ layer is rather weak compared with that of the ZnO layer. As the applied voltage increases, more electrons will gain enough energy, and more electrons can tunnel into the $Mg_{0.39}Zn_{0.61}O$ layer since the effective thickness of the barrier will be decreased further; thus the emission of the $Mg_{0.39}Zn_{0.61}O$ layer will be greatly enhanced. Meanwhile, the electric filed at the ZnO/MgO interface will also be increased so that more and more holes will be evacuated from this region before recombining with deep centers. As a result, the deep-level emissions of the n-ZnO layer are gradually suppressed.

In conclusion, accelerated electron excited UV emissions have been obtained from i–ZnO/n–ZnO structures, in which the i-ZnO layer acts as an electron-accelerating layer and n-ZnO as an active layer, and obvious emission at around 385 nm, which is the typical NBE emission of ZnO, has been observed from the structures, indicating that UV emissions can be realized under the excitation of accelerated electrons in the proposed structure. To obtain shorter wavelength UV emissions, $Mg_{0.39}Zn_{0.61}O$ layer was employed as the active layer, and an emission at around 328 nm has been obtained. The results reported in this Letter reveal that UV emissions can be realized by exciting the wide bandgap semiconductors with accelerated electrons in a solid-state structure. This might be found to be a promising alternative route to a low-cost, small-sized UV light source by bypassing the challenging p-type issue of wide bandgap semiconductors.

This work is supported by the National Basic Research Program of China (2011CB302005), the Natural Science Foundation of China (61177040, 11134009, and 10974197), and the Science and Technology Developing Project of Jilin Province (20111801).

References

1. A. Khan, K. Balakrishnan, and T. Katona, Nat. Photon. **2**, 77 (2008).
2. J. Simon, V. Protasenko, C. Lian, H. Xing, and D. Jena, Science **327**, 60 (2010).
3. S. Nakamura, S. Pearton, and G. Fasol, *The Blue Laser Diodes*, 2nd ed. (Springer, 2000).
4. O. Ambacher, J. Phys. D **31**, 2653 (1998).
5. D. C. Look, B. Claflin, Ya. I. Alivov, and S. J. Park, Phys. Status Solidi A **201**, 2203 (2004).
6. P. Bogusławski and J. Bernhoc, J. Phys. D **56**, 9496 (1997).
7. Y. Taniyasu, M. Kasu, and T. Makimoto, Nature **441**, 325 (2006).
8. T. Jüstel, H. Nikol, and C. Ronda, Angew. Chem., Int. Ed. **37**, 3084 (1998).
9. L. Ozawa and M. Itoh, Chem. Rev. **103**, 3835 (2003).
10. S. Zhao, Z. Xu, F. Zhang, W. Jiang, J. Huang, Y. Wang, and X. Xu, Opt. Lett. **32**, 2094 (2007).
11. K. Watanabe, T. Taniguchi, and H. Kanda, Nat. Mater. **3**, 404 (2004).
12. K. Watanabe, T. Taniguchi, T. Niiyama, K. Miya, and M. Taniguchi, Nat. Photon. **3**, 591 (2009).
13. T. Oto, R. G. Banal, K. Kataoka, M. Funato, and Y. Kawakami, Nat. Photon. **4**, 767 (2010).
14. E. F. Schubert and J. Cho, Nat. Photonics **4**, 735 (2010).
15. Y. Nakajima, A. Kojima, and N. Koshida, Appl. Phys. Lett. **81**, 2472 (2002).
16. Y. Nakajima, T. Uchida, H. Toyama, A. Kojima, B. Gelloz, and N. Koshida, Jpn. J. Appl. Phys. **43**, 2076 (2004).
17. W. Jiang, S. Zhao, Z. Xu, and F. Zhang, Displays **29**, 432 (2008).
18. S. Zhao, Z. Xu, F. Zhang, Y. Wang, G. Ji, and X. Xu, J. Appl. Phys. **106**, 023513 (2009).
19. H. Zhu, C. X. Shan, J. Y. Zhang, Z. Z. Zhang, B. H. Li, D. X. Zhao, B. Yao, D. Z. Shen, X. W. Fan, Z. K. Tang, X. H. Hou, and K. L. Choy, Adv. Mater. **22**, 1877 (2010).